Chemical Geology 366 (2014) 32–41

Contents lists available at ScienceDirect

Chemical Geology

journal homepage: www.elsevier.com/locate/chemgeo

Nanoparticulate pyrite and other nanoparticles are a widespread component of hydrothermal vent black smoker emissions

Amy Gartman *, Alyssa J. Findlay, George W. Luther III

School of Marine Science and Policy, College of Earth Ocean and Environment, University of Delaware, 700 Pilottown Road, Lewes, DE, USA

ARTICLE INFO

Article history:
Received 13 May 2013
Received in revised form 17 December 2013
Accepted 18 December 2013
Available online 22 December 2013

Editor: Carla M. Koretsky

Keywords:
Hydrothermal vent
Black smoker
Nanoparticle
Pyrite
Mid-Atlantic Ridge

ABSTRACT

The presence of nanoparticulate pyrite is reported in hydrothermal emissions from Rainbow, TAG and Snakepit on the Mid-Atlantic Ridge (MAR). When coupled with previously collected data from East Pacific Rise 9°N (EPR) and Lau Basin, these data demonstrate that pyrite nanoparticles are a widespread component of black smoker emissions from hydrothermal vents and are found in significant concentrations at a fast spreading mid-ocean Ridge (EPR), a back-arc basin (Lau Basin), and a slow spreading mid-ocean Ridge (MAR). The maximum percentage of filtered iron emitted as nanoparticulate pyrite was found to be as high as 25%, 10%, and 5%, respectively. As a widespread component of hydrothermal vent emissions, these nanoparticles may be an important source of iron to the world's oceans. Metals such as Cu and Zn are detected in pyrite-containing aggregates at all sites, and chalcopyrite was a component of nanoparticle aggregates at MAR. Iron containing silicate nanoparticles are also identified, and indicate that nanoparticles other than sulfides should also be considered when determining transport implications of hydrothermal vent emissions. The varied morphologies and the presence of different minerals within these nanoparticles provide insight into their formation and stability.

1. Introduction

The amount of hydrothermally emitted iron incorporated into the oceanic budget has been debated. Hydrothermally emitted Fe(II) will rapidly oxidize in the neutrally buoyant plume, resulting in the formation of Fe(III) oxyhydroxides (Rudnicki and Elderfield, 1993). As these oxides precipitate, iron and other metal species are scavenged and removed (German et al., 1990; Feely et al., 1991). Fe(II) is also precipitated in sulfides that form as hot hydrothermal fluids are emitted from the seafloor, and further mix with seawater in the buoyant plume. In studies conducted at the Juan de Fuca vent field, the majority of these metal sulfides have been shown to precipitate within approximately 1.5 km of the hydrothermal vent field (Feely et al., 1994). However, recent evidence suggests that hydrothermal emissions contribute significantly to oceanic iron budgets (Taglibue et al., 2010). The mechanism by which hydrothermally emitted iron may be transported to the larger ocean basin is an area of active research and is likely to involve both organic complexation (Bennett et al., 2008; Sander and Koschinsky, 2011) and nanoparticulate minerals (Yücel et al., 2011).

The precipitation of minerals from hydrothermal fluids is influenced both by cooling, which reduces the saturation state of many minerals, and mixing with ambient seawater, which results in a decrease in pH (due to metal-sulfide precipitation) followed by an increase in pH as ambient seawater and oxidized species interact with hydrothermal fluid (Ding and Seyfried, 2007). Based on a combined experimental and thermodynamic modeling approach, Klevenz et al. (2011) concluded that mixing had a greater influence on particle precipitation than conductive cooling. Hydrothermal black smokers exhibit rapid mixing of hot (~350 °C), anoxic vent fluid laden with reduced metals and sulfur, and depleted in sulfate and magnesium, into ambient oxic bottom water. This mixing results in the precipitation of bulk sulfide and silicate minerals, and yields the formation of characteristic hydrothermal vent chimneys (Tivey, 2007).

Nanoparticulate minerals are increasingly recognized as widespread in areas where rates of nucleation exceed rates of growth, and hydrothermal vents may be a prime example of this type of location (Hochella et al., 2008). Nanoparticles are defined as particles with one or more dimensions less than 100 nm in size, and their identification in the ocean alters previous paradigms on mineral transport and stability. Insoluble metal sulfides and oxides may achieve oceanic transport as nanoparticles, since nanoparticles do not settle out of seawater rapidly (Yücel et al., 2011). In addition, nanoparticles may behave differently than bulk species with regard to oxidation, requiring revised assumptions about particle lifetimes and reactivity (Hochella et al., 2008). Several recent studies have identified nanoparticles in hydrothermal emissions, including Yücel et al. (2011), who identified pyrite nanoparticles in high temperature black smoker fluid at Lau Basin; Hsu-Kim et al. (2008) who identified ZnS nanoparticles and clusters at Lau Basin; and Kadar et al. (2012) who identified numerous metallic

Abbreviations: EPR, East Pacific Rise 9°N; MAR, Mid-Atlantic Ridge; MORB, Mid-Ocean Ridge Basalt; ROV, Remotely Operated Vehicle; XRD, X-Ray Diffraction; SEM, Scanning Electron Microscopy; EDX, Energy Dispersive X-Ray Spectroscopy; TEM, Transmission Electron Microscopy; EELS, Electron Energy Loss Spectroscopy; AVS, Acid Volatile Sulfide; CRS, Chromium Reducible Sulfide.

* Corresponding author. Tel.: +1 914 213 3085.
E-mail address: agartman@udel.edu (A. Gartman).

0009-2541/$ – see front matter © 2013 Elsevier B.V. All rights reserved.
http://dx.doi.org/10.1016/j.chemgeo.2013.12.013

Table 1
Fe(II) and sulfide data for samples shown in Fig. 1. S_{Total} is AVS + CRS. Nanoparticulate pyrite, for samples in which it was detected is given both as a percent and as a concentration. No Fe(III) was detected in any of these samples. The p-value is based on a two-tailed type 1 *t*-test between the HCl and HNO_3 values, showing that they are significantly different.

Site	Sample	T (°C)	pH	Fe_{py} (mM)	Fe_{py} %	p-value	Fe_{Total} (mM)	S_{Total} (mM)
Rainbow	R1	367	3.28	ND	–	–	17.6 ± 0.788	0.60 ± 0.60
	R2	353	5.34	ND	–	–	3.80 ± 0.636	0.037 ± 0.0043
	R3	368	4.65	ND	–	–	9.27 ± 142	0.24 ± 0.045
	R4	367	2.87	1.15	5.24	0.08	22.4 ± 0.748	0.50 ± 0.17
	R5	371	3.16	ND	–	–	21.8 ± 0.171	0.17 ± 0.054
	R6	230	3.37	ND	–	–	15.2 ± 0.224	0.16 ± 0.039
TAG	T1	303	4.56	ND	–	–	1.73 ±0.0129	0.46 ± 0.17
	T2	302	3.20	0.234	4.83	0.06	4.90 ± 0.0641	1.3 ± 0.33
	T3	313	3.03	ND	–	–	4.84 ± 0.0900	1.6 ± 0.18
	T4	355	4.80	ND	–	–	1.47 ± 0.0414	0.29 ± 0.13
	T5	310	2.98	0.199	4.02	0.02	5.06 ± 0.0169	2.8 ± 0.55
	T6	366	3.14	ND	–	–	5.06 ± 0.114	2.9 ± 0.36
	T7	347	5.11	0.0354	2.86	0.04	1.07 ± 0.0111	0.23 ± 0.033
	T8	365	3.01	ND	–	–	5.08 ± 0.0778	2.0 ± 0.42
	T9	189	4.15	0.0511	2.01	0.06	2.29 ± 0.0150	ND
	T10	360	4.92	0.0376	2.77	0.0002	1.25 ± 0.00203	0.38 ± 0.092
	T11	347	3.38	0.0255	0.83	0.05	2.68 ± 0.00947	0.24 ± 0.077
Snakepit	Beehive 4	340	5.17	ND	–	–	0.359 ± 0.0051	0.50 ± 0.027
	Beehive 9	358	4.42	0.0350	2.66	0.07	0.891 ± 0.0196	0.68 ± 0.24
	Beehive 7	347	3.22	ND	–	–	2.58 ± 0.146	0.74 ± 0.079
	Beehive 8	351	3.45	ND	–	–	3.60 ± 0.0883	0.74 ± 0.068
	Beehive 2	342	3.29	0.0962	2.81	0.02	3.36 ± 0.0966	2.0 ± 0.18
	Moose 3	336	3.19	ND	–	–	3.20 ± 0.123	0.63 ± 0.043

nanoparticles in CO_2 seeps in the Mediterranean. Sands et al. (2012) investigated the distribution of different metals between the dissolved, colloidal and particulate phases in a non-buoyant hydrothermal plume and identified significant iron in all three phases. It is likely that more examples of nanoparticles in hydrothermal emissions will be found as further studies considering them are conducted. The impact that iron emitted as nanoparticulate pyrite will have as an iron source to the larger ocean is likely to depend as much on bottom water currents and deep water chemistry affecting particle oxidation at a given vent site, as on the concentration of nanoparticulate pyrite emitted at that vent site. These processes have been previously discussed as influencing Fe(II) distributions (Field and Sherrell, 2000).

Due to the rapid fluid emissions and mineralization reactions that occur at hydrothermal vents, this study aims to demonstrate that pyrite and other nanoparticles are a widespread component of black smoker emissions. To demonstrate that these particles are widespread in

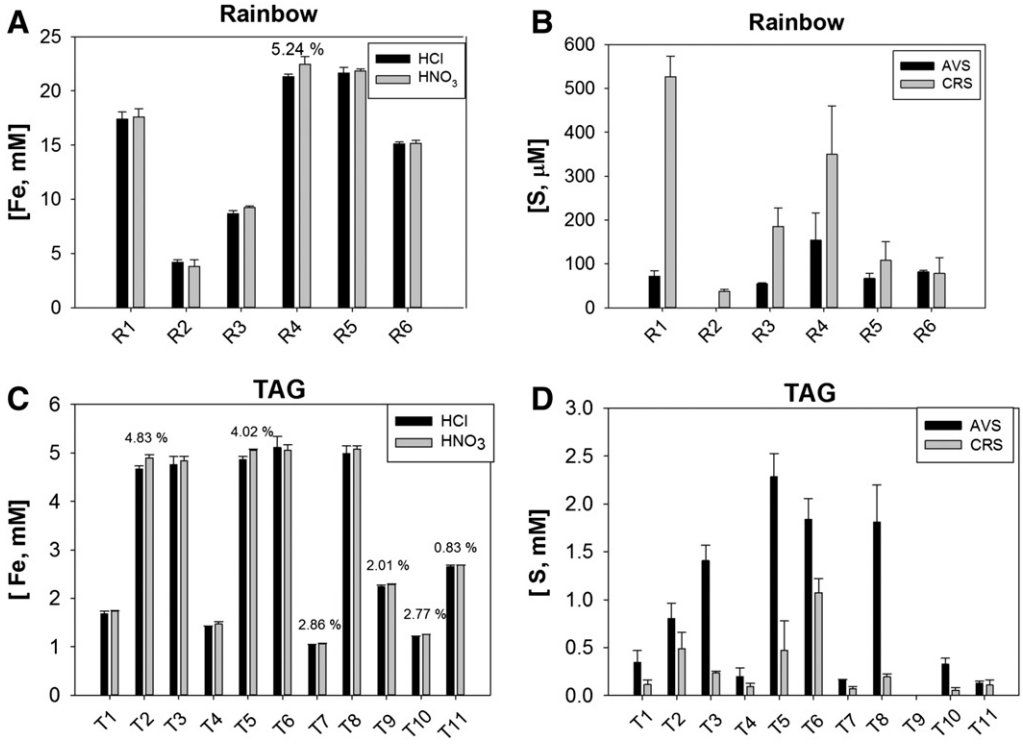

Fig. 1. HCl/HNO_3 soluble iron and AVS/CRS results for all 0.2 µm filtered samples, including those that did not contain significant nanoparticulate pyrite. Samples containing nanoparticulate pyrite are noted above columns A, C and E, as the percent of total sub-0.2 µm Fe(II) present as pyrite. Total Fe(II), sulfide and Fe_{py} are also listed in Table 1. Samples shown were collected at the following locations A–B. Rainbow. Samples at Rainbow are from chimneys 6, 7, and 9 identified in the Flores cruise (In Fig. 1b of Charlou et al., 2002). C–D. TAG. All samples from TAG are from the black smoker complex at the top of the TAG mound (Tivey et al., 1995). E–F. Snakepit. Beehive and Moose are two black smoker clusters at Snakepit (described in Section 1). G–H. EPR 9°N. Only one of the two samples collected from EPR 9°N in 2012 was fixed for sulfide analysis.